

# Rare Earth-Doped Nanocrystals for Biosensing and Imaging

by Dhiraj K. Sardar, Kelly L. Nash and John B. Gruber, University of Texas at San Antonio, and Anthony Sayka, Maxim Integrated Products

## Synthesis and optical characterization of $\text{Er}^{3+}:\text{Y}_2\text{O}_3$ nanocrystals show their potential.

There has been a great deal of interest in the fabrication and characterization of highly luminescent nanoparticles because of their potential applications as nanosensors and as biosensors for applications such as molecular diagnostics. The organic dyes currently used in biomedical applications of imaging and immunoassays have advantages such as commercial availability and high quantum yield, but they also have disadvantages such as broad spectral band, short fluorescence lifetime and photobleaching.

In contrast, rare-earth (RE) nanoparticles exhibit sharp line emission bands, reasonably large Stokes shifts and long fluorescence lifetimes, and they can be encapsulated in neutral environments to avoid toxic reactions. In addition, rare-earth nanoparticles have a high quantum yield and excellent photostability. These nanoparticles can enable time-resolved fluorescence imaging for quantitative detection of antigens as well as tissue-specific transcripts and genes. They have the potential to be used for noninvasive, non-destructive and real-time in vivo diagnosis of various diseases, including atherosclerotic plaques, which can lead to stroke and heart disease.<sup>1</sup>

Optimized rare earth-based nanoparticles could be useful for nanosensors, bioprobes, drug discovery, medical diag-

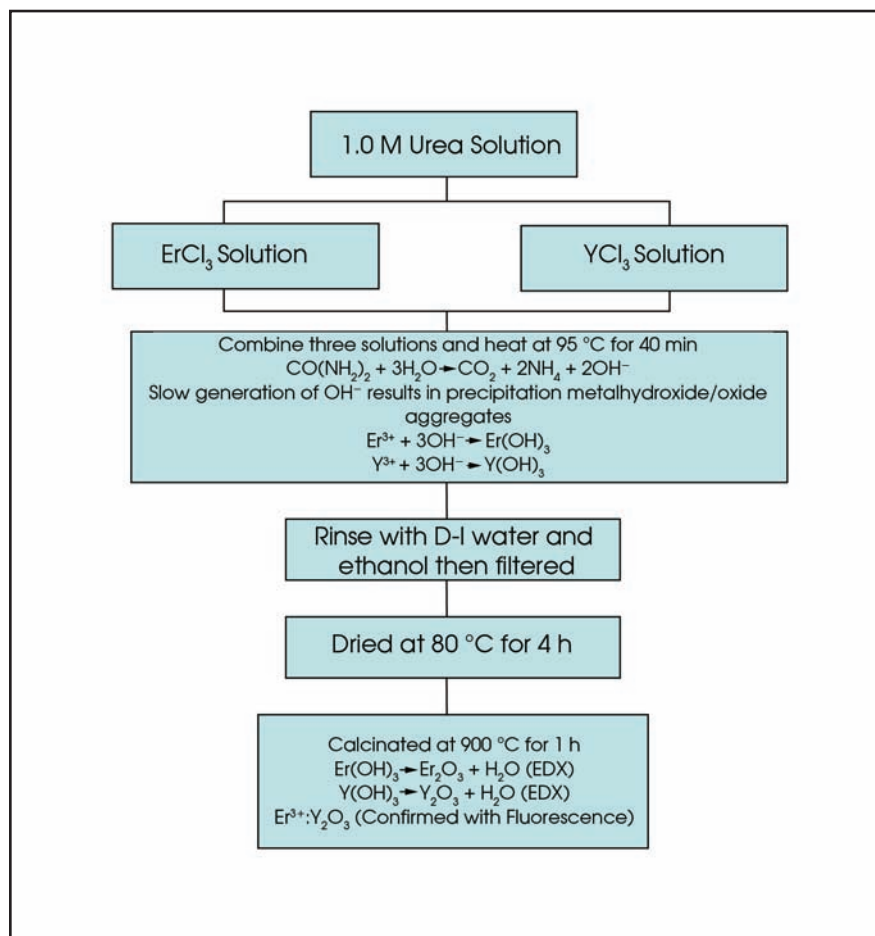


Figure 1. An overview of  $\text{Er}^{3+}:\text{Y}_2\text{O}_3$  nanocrystal synthesis is shown.

nostics, genetic analysis, flow cytometry and high-throughput screening. Because their emission wavelength has been shown to be independent of particle size, they may be tailored for applications with dimensional constraints without altering the optical characterization of the nanoparticles. Thus nanometer- and micrometer-size phosphors made of rare earth-doped metal oxides are promising for use as a luminescent tag or reporter for affinity or immunoassays in biomedical, environmental, food quality and drug testing probes.

The large Stokes shift of the nanoparticles enables subtraction of the excitation wavelength by filtering, while the long lifetime enables time-gated detection and subtraction of the background autofluorescence. In addition, the nanoparticles permit the use of near-infrared upconversion excitation to avoid autofluorescence completely. Particles with various emission spectra can be obtained by controlled doping of rare-earth ions into an appropriate matrix.<sup>2</sup> A rapid and inexpensive method of preparing luminescent nanoparticles of europium oxide has been demonstrated recently by using a microwave-assisted surface chemistry.<sup>3</sup>

According to W.O. Gordon et al, the small size of luminescent inorganic nanoparticles allows rare-earth ions to replace fluorescent molecules or complexes in analytical applications.<sup>4</sup> Also, different lanthanide ions doped with gadolinium oxide  $Gd_2O_3$  nanoparticles demonstrate host and dopant combinations with a common excitation wavelength that can be used for multicolor immunoassays.<sup>5</sup> Thus, the potential for application of the inorganic labels is very promising if full use is made of the unique optical properties of these rare earth-based nanoparticles.

We studied trivalent erbium  $Er^{3+}$  as a dopant for these nanoparticles because of its strong, narrow absorption and emission lines in the visible to near-infrared region. We synthesized erbium-doped yttrium-oxide ( $Er^{3+}:Y_2O_3$ ) nanoparticles and performed spectroscopic analyses to demonstrate their usefulness.

### Synthesis and analysis

$Er^{3+}$  and  $Nd^{3+}$  nanocrystals doped into  $Y_2O_3$  are prepared by a precipitation of select rare-earth salts in a urea solution.<sup>6, 7, 8</sup> Maria Pires et al have shown that varying the concentration of the rare-earth materials controls the size and shape of the resulting nanocrystals.<sup>11</sup> Our studies showed that a 40:60 ratio of  $RECl_3$  to  $YCl_3$  is optimal. We prepared the nanocrystals

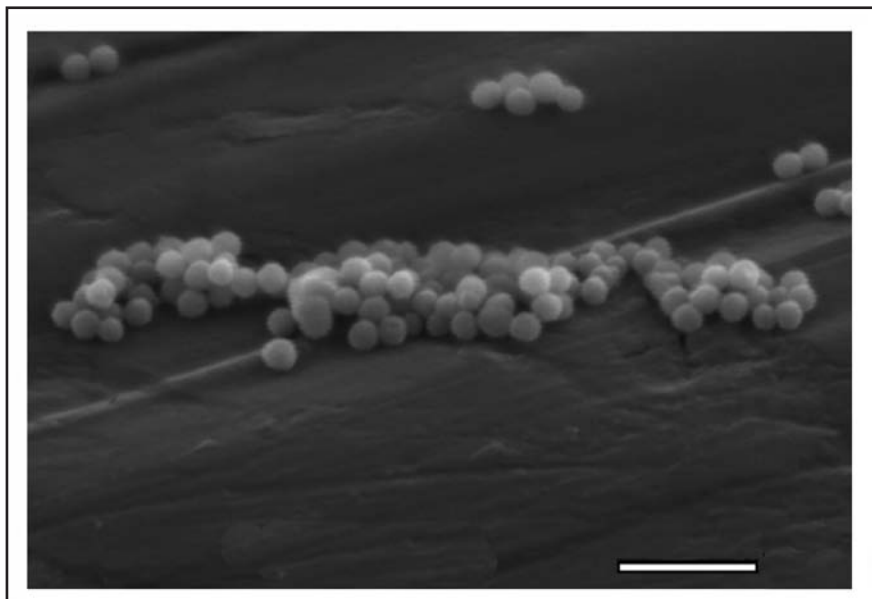


Figure 2. This scanning electron micrograph reveals  $Er^{3+}:Y_2O_3$  nanoparticles.

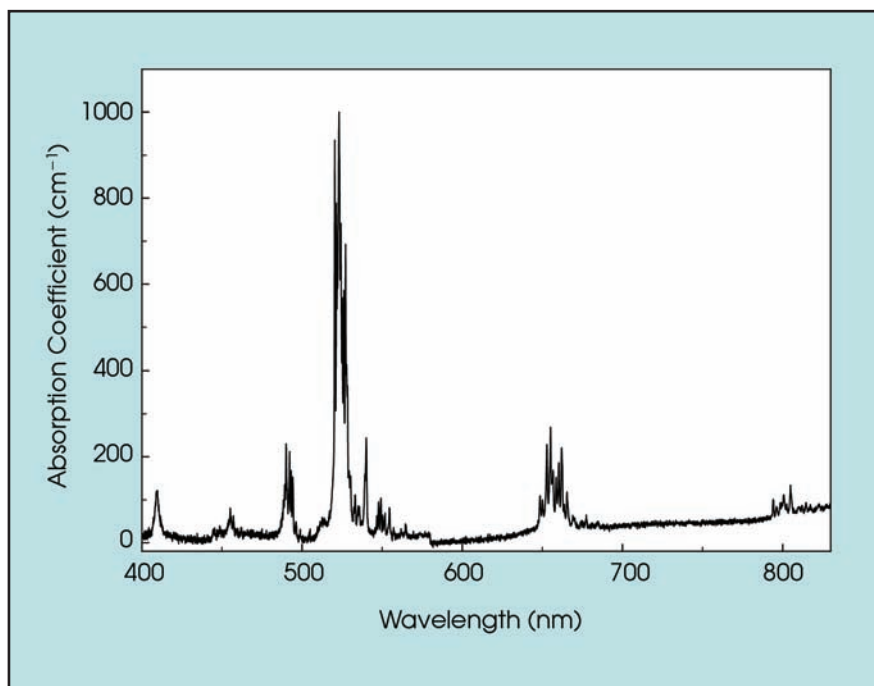


Figure 3. Depicted is the absorption spectrum of  $Er^{3+}:Y_2O_3$  nanoparticles at room temperature.

from a homogeneous solution of dissolved  $\text{RECl}_3$  and  $\text{YCl}_3$  and urea using a slow precipitation method. An overview of the nanocrystal synthesis is provided in Figure 1.

A generation of  $\text{OH}^-$  ions comes from the decomposition of urea, as the solution is heated and stirred at  $95^\circ\text{C}$  for 40 minutes. The slow generation of the hydroxide ions in a homogeneous solution results in a precipitation of aggregates of mixed metal hydroxide/oxide nanoparticles. The precipitates are filtered from the solution, washed with distilled water and ethanol, dried at  $80^\circ\text{C}$  and then calcinated at  $900^\circ\text{C}$  for more than an hour to convert all solid material to the oxide form. Our method of preparation is inexpensive.

We measured the presence and the relative amount of erbium and neodymium in the yttrium-oxide nanocrystals using energy-dispersive x-ray analysis. Sampling various sites yielded an atomic weight percentage of 6 to 10 percent atomic weight for the  $\text{Er}^{3+}$ -doped  $\text{Y}_2\text{O}_3$  prepared using the 40:60 ( $\text{ErCl}_3$ : $\text{YCl}_3$ ) ratio.

Scanning electron microscopy images revealed that the  $\text{Er}^{3+}$ : $\text{Y}_2\text{O}_3$  aggregates are uniform in size and spherical in shape, and the aggregated particles are  $\sim 150$  to  $200$  nm in size (Figure 2).

The x-ray diffraction pattern revealed that the  $\text{Er}^{3+}$ : $\text{Y}_2\text{O}_3$  nanocrystals have a cubic structure comparable to that of single-crystal  $\text{Y}_2\text{O}_3$ , with a lattice constant of approximately  $10.59$ . Using the diffraction data, we used the Debye-Scherrer equation to calculate the smallest crystalline sizes of the  $\text{Er}^{3+}$ : $\text{Y}_2\text{O}_3$  sample. The strongest peak, which corresponds to the (222) crystallographic plane, was analyzed to obtain an average particle size of  $29$  nm for the  $\text{Er}^{3+}$ : $\text{Y}_2\text{O}_3$  nanocrystals.

### Optical measurements

The room temperature absorption spectrum of  $\text{Er}^{3+}$ : $\text{Y}_2\text{O}_3$  nanoparticles showed that they had sharp absorption peaks that were comparable to those of  $\text{Er}^{3+}$  doped into pure crystals. The sharp line structure of the absorption spectrum shown in Figure 3 comes from transitions from the ground state of the  $\text{Er}^{3+}$  ion to the numerous excited state energy levels of  $\text{Er}^{3+}$  that are split by the crystal field established by the sublattices of the oxygen ions in the  $\text{Y}_2\text{O}_3$  crystal. These levels can be pumped directly by diode array laser sources emitting at the same wavelength as the  $\text{Er}^{3+}$  ion absorbs to provide emission at various wavelengths suitable for numerous applications.

Judd-Ofelt analysis also was performed to provide critical spectroscopic and laser

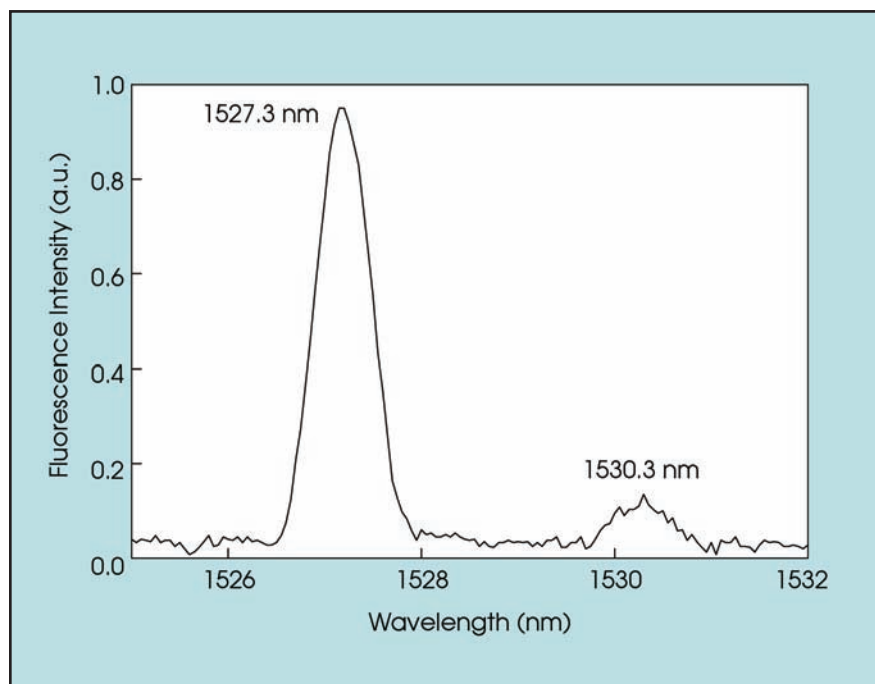


Figure 4. The room temperature fluorescence spectrum of  $\text{Er}^{3+}$ : $\text{Y}_2\text{O}_3$  nanoparticles is shown.

parameters such as radiative lifetime rates and quantum efficiency. The model uses absorption bands in the room temperature absorption spectrum that resulted in three phenomenological intensity parameters:  $\Omega_2 = 4.13 \times 10^{-20} \text{ cm}^2$ ,  $\Omega_4 = 1.43 \times 10^{-20} \text{ cm}^2$ , and  $\Omega_6 = 1.18 \times 10^{-20} \text{ cm}^2$  for  $\text{Er}^{3+}:\text{Y}_2\text{O}_3$  nanoparticles. These values are comparable to those obtained for  $\text{Er}^{3+}:\text{Y}_2\text{O}_3$  single crystal.<sup>10</sup> Following the Judd-Ofelt analysis, the radiative lifetime of the  $^4\text{I}_{13/2} \rightarrow ^4\text{I}_{15/2}$  (1.5  $\mu\text{m}$ ) transition was determined to be approximately 48 ms, and the fluorescence lifetime was measured to be 45 ms, giving rise to the quantum efficiency of about 99 percent.

This lifetime is much longer than the lifetime measured on the same transition of  $\text{Er}^{3+}$  in other oxide hosts. We have calculated an even longer lifetime (~60 ms) using the values of the  $\Omega_n$  parameters reported by W.F. Krupke<sup>9</sup> for the  $^4\text{I}_{13/2} \rightarrow ^4\text{I}_{15/2}$  transition in bulk crystals of  $\text{Er}^{3+}:\text{Y}_2\text{O}_3$ . Such a result suggests merit in attempting resonant diode pumping of these cubic nanoparticle crystals for stimulated emission at 1.5  $\mu\text{m}$ .

The room temperature fluorescence spectrum of the  $\text{Er}^{3+} \ ^4\text{I}_{13/2} \rightarrow ^4\text{I}_{15/2}$  (~1.5  $\mu\text{m}$ ) intermanifold transition is shown in Figure 4. This spectrum was recorded using a 1.2-m Jobin Yvon monochromator and exciting the  $\text{Er}^{3+}:\text{Y}_2\text{O}_3$  nanoparticle with the 488-nm line from an argon-ion laser. The laser power was kept at 280 mW during the measurement. The slit width of the monochromator was 0.5 mm. This part of the fluorescence spectrum is particularly interesting because it shows the large Stokes shift relative to the excitation source and appears in the wavelength region of particular importance for biomedical studies and applications.

Our studies show that  $\text{Er}^{3+}:\text{Y}_2\text{O}_3$  nanoparticles, which can be used as a luminescent tag or reporter for immunoassays, possess sharp and strong emission at the near-infrared region with a long lifetime. The long lifetime of  $\text{Er}^{3+}$  doped in a  $\text{Y}_2\text{O}_3$  nanoparticle provides a significant advantage in discriminating its fluorescence from the background autofluorescence. Furthermore, the nanoparticles have potential for in vivo imaging and in vivo biosensors.

In a recent publication, M.K. So et al demonstrated covalent linking of quantum dots to a bioluminescent protein to create "self-illuminating" particles.<sup>10</sup> We believe that rare earth-based nanoparticles will be amenable to a similar adaptation. Thus, a very promising application of the optical properties of rare-earth nanoparticles appears ahead.  $\square$

## Acknowledgments

This work has been supported by the NSF-sponsored Center for Biophotonics Science and Technology at the University of California, Davis. The authors would like to thank Kevin Taylor and Robert Splinter at Spectranetics Corp. in Colorado Springs, Colo., for their invaluable suggestions.

## Meet the authors

Dhiraj K. Sardar is a professor of physics at the University of Texas at San Antonio; e-mail: dsardar@utsa.edu.

Anthony Sayka is currently employed by Maxim Integrated Products Inc. in San Antonio; e-mail: saykacr@hotmail.com.

John B. Gruber is a research professor at University of Texas at San Antonio; e-mail: johnbgruber@yahoo.com.

Kelly L. Nash is pursuing a PhD in physics at the University of Texas at San Antonio; e-mail: knash@lonestar.utsa.edu.

## References

1. D. Dosi et al (November-December 2005). Application of luminescent  $\text{Eu}:\text{Gd}_2\text{O}_3$  nanoparticles to the visualization of protein micropatterns. *J BIO-MED OPT*, pp. 1-7.
2. B.M. Tissue (October 1998). Synthesis and luminescence of lanthanide ions in nanoscale insulating hosts. *J CHEM MATER*, pp. 2837-2845.
3. J. Feng et al (Oct. 1, 2003). Functionalized europium oxide nanoparticles used as a fluorescent label in an immunoassay for atrazine. *J ANAL CHEM*, pp. 5282-5286.
4. W.O. Gordon et al (June 2004). Long-lifetime luminescence of lanthanide-doped gadolinium oxide nanoparticles for immunoassays. *J LUMIN*, pp. 339-342.
5. J.B. Gruber et al (July 19, 2007). Comparative study of the crystal-field splitting of trivalent neodymium energy levels in polycrystalline ceramic and nanocrystalline yttrium oxide. *J APPL PHYS*, 023103.
6. D.K Sardar et al (June 15, 2007). Absorption intensities and emission cross sections of intermanifold transition of  $\text{Er}^{3+}$  in  $\text{Er}^{3+}:\text{Y}_2\text{O}_3$  nanocrystals. *J APPL PHYS*, 113115.
7. J.B. Gruber (June 15, 2007). Spectral analysis of synthesized nanocrystalline aggregates of  $\text{Er}^{3+}:\text{Y}_2\text{O}_3$ . *J APPL PHYS*, 113116.
8. Maria Pires et al (June 2005). Morphological and luminescent studies on nanosized Er, Yb-Yttrium oxide up-converter prepared from different precursors. *J LUMIN*, pp. 174-182.
9. W.F. Krupke (1966). Optical absorption and fluorescence intensities in

several rare-earth-doped  $\text{Y}_2\text{O}_3$  and  $\text{LaF}_3$  single crystals. *PHYS REV*, pp. 325-337.

10. M.K. So et al (Feb. 16, 2006). Self-illuminating quantum dot conjugates for in vivo imaging. *NAT BIOTECH*, pp. 339-343.